Large scale flows under location uncertainty: a consistent stochastic framework

Bertrand Chapron, Pierre Dérian, Etienne Mémin, Valentin Resseguier

Large scale flows under location uncertainty: a consistent stochastic framework

B. Chapron, [a], P. Dérian, [b], E. Mémin,[b]*, V. Resseguier,[ab]

[a] *Ifremer, LOPS, Pointe du Diable, Plouzané 29280, France*

[b] *Inria/Irmar, Fluminance, Campus universitaire de Beaulieu, Rennes Cedex 35042, France*

Using a classical example, the Lorenz-63 model, an original stochastic framework is applied to represent large-scale geophysical flow dynamics. Rigorously derived from a reformulated material derivative, the proposed framework encompasses several meaningful mechanisms to model geophysical flows. The slightly compressible set-up, as treated in the Boussinesq approximation, brings up a stochastic transport equation for the density and other related thermo-dynamical variables. Coupled to the momentum equation through a forcing term, a resulting stochastic Lorenz-63 model is consistently derived. Based on such a reformulated model, the pertinence of this large-scale stochastic approach is demonstrated over classical eddy-viscosity based large-scale representations.

Key Words: Large scale flow modeling, Stochastic parameterization, Modeling under location uncertainty, Stochastic Lorenz model,Stochastic transport

Received . . .

1. Introduction

Today, in their most common expression, large-scale geophysical flow representations rely on the Reynolds decomposition and the inclusion of a subgrid dissipative model to represent the action of numerically non-resolved components over the resolved scales. Most used subgrid models heavily bank on the *eddy viscosity* concept – also called Boussinesq assumption (Boussinesq 1877) – built upon a straight analogy with the molecular dissipation mechanism. The celebrated Smagorinsky model (Smagorinsky 1963) is one of the most representative instance of such models. The *eddy viscosity* concept is essential to achieve a numerical stability in draining the energy accumulated at the cutoff resolution through the direct energy cascade process. Its pure dissipative behavior further prevent to take into account local backscattered energy or inhomogeneous turbulence.

To represent the large-scale evolution of turbulent fluid flows, a different strategy can be envisaged, considering the decomposition of the flow into a large-scale smooth component and a fast oscillating velocity component modeled as a random field (seen as decorrelated at large scales). Yet, such a decomposition requires to modify the material derivative through the introduction of a stochastic transport operator (Mémin 2014; Resseguier *et al.* 2017a).

One advantage of this framework over the Reynolds decomposition lies in its ability to deal with non-smooth expressions of the small-scale component at the resolved time scale. It further introduces, without any supplementary assumption, the following mechanisms: (*i*) a dissipative operator directly related to the mixing effect of the large-scale components by the small-scale velocity; (*ii*) a multiplicative noise representing small-scale energy backscattering; and (*iii*) a modified advection term related to the so-called *turbophoresis* phenomena, associated to the migration of inertial particles in regions of lower turbulent diffusivity (Reeks 1983). Those properties have already been used to define data-driven inhomogeneous subgrid models to stabilize reduced order flow models in capturing the principal local dissipation directions and the small-scale induced advection field (Resseguier *et al.* 2017d). Corresponding eddy-viscosity models are not any more constant, but adapted to the dynamics. This random framework also enables to derive stochastic dynamics from the very same physical conservation principles as in the deterministic case and is amenable to the usual geophysical scaling approximations (Resseguier *et al.* 2017b,c).

In this work, this representation is applied to the famous Lorenz-63 model to illustrate the pertinence of such a consistent stochastic representation over a classical eddy diffusivity model. In particular, it is shown for the Lorenz-63 that a classical eddy-viscosity modelling strongly slows down the exploration of the attractor, while the stochastic approach provides a much faster exploration.

2. Stochastic representation of the Lorenz-63 model

The celebrated Lorenz-63 model (Lorenz 1963) corresponds to the description of an incompressible flow undergoing a Rayleigh-Bénard convection caused by a temperature gradient between the bottom and the top of the fluid domain. It aims at representing atmospheric convection in a 2D simplified way.

The Lorenz-63 model is formally derived from the Boussinesq approximation – i.e. small density variations – of the Navier-Stokes equations. Its complete derivation is described in Lorenz original paper (Lorenz 1963) or given in greater details in the book Berge *et al.* (1987). To derive its stochastic representation, we closely follow the same derivation. Yet, we start from a stochastic Boussinesq system, derived itself from physical conservation principles and a stochastic representation of the flow. Such representation, termed as modeling under location uncertainty, has been recently proposed in Mémin (2014); Resseguier *et al.* (2017a), and is hereafter outlined. Note that similar models could be derived from Hamiltonian principles as described in Holm (2015).

2.1. Flow modeling under location uncertainty

In the modeling under uncertainty the model errors are introduced at the lowest level of the dynamics. The basic idea is built on the assumption that the Lagrangian fluid particles displacement, $\boldsymbol{X}_t$, results from a smooth velocity component, $\mathbf{v}$, and a fast oscillating random field uncorrelated in time. At time t, the location of a fluid particle initially located at $\boldsymbol{X}_{t_0}$ is:

$$\boldsymbol{X}_t = \boldsymbol{X}_{t_0} + \int_{t_0}^{t} \mathbf{v}(X_s, s)\mathrm{d}s + \int_{t0}^{t} \boldsymbol{\sigma}(X_s, s)\mathrm{d}\boldsymbol{B}_s, \tag{1}$$

which reads also in a more compact differential form as:

$$\mathrm{d}\boldsymbol{X}_t = \mathbf{v}(\boldsymbol{X}_t, t)\mathrm{d}t + \boldsymbol{\sigma}(\boldsymbol{X}_t, t)\mathrm{d}\boldsymbol{B}_t. \tag{2}$$

The solenoidal (possibly inhomogeneous) random field, representing the small-scale velocity component, is build through the application of a linear operator, $\boldsymbol{\sigma}$, to a space-time white noise, $\mathrm{d}\boldsymbol{B}_t$. It is explicitly defined on a spatial domain Ω from a kernel, $\breve{\boldsymbol{\sigma}}$, as:

$$\boldsymbol{\sigma}(\boldsymbol{x},t)\mathrm{d}\boldsymbol{B}_t = \int_\Omega \breve{\boldsymbol{\sigma}}(\boldsymbol{x},\boldsymbol{y},t)\mathrm{d}\boldsymbol{B}_t(\boldsymbol{y})\mathrm{d}\boldsymbol{y}. \tag{3}$$

The kernel, $\breve{\boldsymbol{\sigma}}$, (or the operator $\boldsymbol{\sigma}$) encodes the random field spatial correlations, whereas the white noise function specifies its temporally decorrelated character.

Decomposition (2) leads to a stochastic representation of both the Reynolds transport theorem (RTT) and the material derivative, D_t (derivative along the flow). When the material derivative of a quantity is deterministic, (such as in the case of a conservation constraint, for instance) this derivative coincides with the stochastic transport operator, $\mathbb{D}_t$, defined for any field Θ as:

$$\mathbb{D}_t\Theta = \mathrm{d}_t\Theta + \left(\mathbf{v}^\star \mathrm{d}t + \boldsymbol{\sigma}\mathrm{d}\boldsymbol{B}_t\right)\cdot\boldsymbol{\nabla}\Theta - \boldsymbol{\nabla}\cdot\left(\frac{1}{2}\boldsymbol{a}\boldsymbol{\nabla}\Theta\right)\mathrm{d}t, \tag{4}$$

involving the time increment term $\mathrm{d}_t\Theta = \Theta(\boldsymbol{x},t+\mathrm{d}t) - \Theta(\boldsymbol{x},t)$, as Θ is a non differentiable random function. This function depends among other things on the particles driven by the Brownian component flowing through a given point. The diffusion matrix, $\boldsymbol{a}$, is solely defined by the one-point one-time covariance of the unresolved displacement per unit of time:

$$\boldsymbol{a}(\boldsymbol{x},t) = \boldsymbol{\sigma}(\boldsymbol{x},t)\boldsymbol{\sigma}(\boldsymbol{x},t)^T = \frac{\mathbb{E}\left\{\boldsymbol{\sigma}(\boldsymbol{x},t)\mathrm{d}\boldsymbol{B}_t\left(\boldsymbol{\sigma}(\boldsymbol{x},t)\mathrm{d}\boldsymbol{B}_t\right)^T\right\}}{\mathrm{d}t}. \tag{5}$$

This quantity corresponds to the diagonal of the covariance tensor and has the dimension of an eddy viscosity term (with units in $\mathrm{m}^2\mathrm{s}^{-1}$). The modified drift is given by

$$\mathbf{v}^\star = \mathbf{v} - \frac{1}{2}(\boldsymbol{\nabla}\cdot\boldsymbol{a})^T. \tag{6}$$

As derived, both the stochastic RTT and material derivative involve a diffusive subgrid term, a multiplicative noise and a modified advection drift induced by the small-scale inhomogeneity. This material derivative has the remarkable property to conserve the energy of any randomly transported tracer realization (Resseguier *et al.* 2017a):

$$\frac{\mathrm{d}}{\mathrm{d}t}\int_\Omega \Theta^2 = \int_\Omega \mathbb{D}_t\Theta^2 = 0. \tag{7}$$

Given the RTT, the classical conservation laws of mechanics (linear momentum, energy, mass) can be expressed within a stochastic flow of form (2). It should be noted that an incompressible homogeneous noise, *i.e.* with a divergence-free diffusion tensor $\boldsymbol{\nabla}\cdot\boldsymbol{\sigma}(\boldsymbol{x},t) = 0$, defined over a periodic domain for simplicity, leads to a constant diffusion matrix. In that case, the effective advection reduces to the large-scale drift component, and the diffusive subgrid term boils down to weighted second order partial derivatives.

The modeling under location uncertainty thus conveys a practical alternative to the design of stochastic representations for geophysical flows. Various techniques have already been considered such as homogeneization, stochastic modes reduction, renormalization closure, a posteriori random forcing, or parameter random perturbation (see Berner *et al.* (2017); Franzke *et al.* (2015) and references therein for a review). However, the modeling under location uncertainty unambiguously provides a rigorous physical derivation of the stochastic system that directly stems from the conservation principles. It then facilitates the set-up of classical

scaling procedures to include all the ingredients needed for a large scale representation, e.g. subgrid diffusion, modified advection akin to *turbophoresis* phenomenon and backscattering. To obtain similar stochastic Eulerian equations, Holm (2015) relies on geometric mechanics and a variational principle to propose an alternative construction. This latter formulation is helicity preserving, whereas the modeling under uncertainty conserves the energy. Those stochastic models have been recently justified through the homogeneization of multiscale Lagrangian dynamics Cotter *et al.* (2017), and when restricted to a 3D (energy conserving) Euler model, Crisan *et al.* (2017) demonstrates that analytical properties of the 3D deterministic Euler equations are also preserved by such stochastic representations.

2.2. *Boussinesq system under location uncertainty*

Following the location uncertainty principle, stochastic Navier-Stokes and Boussinesq models have been derived by Mémin (2014) and Resseguier *et al.* (2017a), respectively. In a 2D inertial frame of reference indexed by the horizontal and vertical coordinates x and z, an incompressible anisotropic homogeneous random field (*i.e.* with $\boldsymbol{\nabla}\cdot\breve{\boldsymbol{\sigma}}(\boldsymbol{x}-\boldsymbol{x}')=0$) is characterized by a constant diagonal diffusion tensor $\boldsymbol{a}=\mathrm{diag}(\mathrm{a_x},\mathrm{a_z})$. Accordingly, the momentum equation of the large scale velocity $\mathbf{v}=(u,w)^T$ reads:

$$\rho\big(\partial_t\mathbf{v}+(\mathbf{v}\cdot\boldsymbol{\nabla})\mathbf{v}-\frac{1}{2}\sum_i a_i\partial^2_{ii}\mathbf{v}\big)=\rho\boldsymbol{g}-\boldsymbol{\nabla}P+\mu\boldsymbol{\nabla}^2\mathbf{v}, \tag{8}$$

where with usual notations μ denotes the dynamic viscosity, P is the pressure, and $\boldsymbol{g}$ the gravity force. Thanks to the homogeneous structure of the noise component, these equations closely resemble a large-scale model with proper constant eddy viscosity coefficients along the horizontal and vertical directions. Yet, this system is complemented by a stochastic thermo-dynamical equation describing the temperature evolution:

$$\mathbb{D}_tT=D_T\Delta T\mathrm{d}t. \tag{9}$$

As previously discussed (7), when the thermal diffusion coefficient D_T is negligible, the temperature is transported and its norm is preserved. In the steady non-convective state (when the fluid is at rest), the temperature varies linearly with the domain depth h: $T(x,z,t)=T_b-\frac{z}{h}\delta T$, where $\delta T=T_b-T_u$ is positive as the bottom temperature T_b is higher than the temperature at the top T_u. The deviation from this linear model is:

$$\tau(x,z,t)=T(x,z,t)-T_b+\frac{z}{h}\delta T, \tag{10}$$

and its evolution obeys the following stochastic evolution law:

$$\mathbb{D}_t\tau-w\frac{\delta T}{h}\mathrm{d}t-\frac{\delta T}{h}(\boldsymbol{\sigma}\mathrm{d}\boldsymbol{B}_t)_z=D_T\nabla^2\tau\mathrm{d}t. \tag{11}$$

This latter model introduces a random transport of the temperature fluctuation, together with deterministic and random forcing of the vertical velocity component. Writing the density variations in power of temperature fluctuation $(T-T_b)$, to leading order we may write $\rho(T)=\rho_0-\alpha\rho_0\left[-\frac{z}{h}\delta T+\tau\right]$, where $\rho_0=\rho(T_b)$ and the thermal expansion coefficient is $\alpha=-\frac{1}{\rho_0}\frac{\partial\rho}{\partial T}$. Under the assumption of negligible compressibility, the Boussinesq approximation states that the density variations can be ignored in the momentum equation (8) and only kept within the gravity term. This system further simplifies through the hydrostatic equilibrium, which holds for the fluid at rest:

$$\partial_t\mathbf{v}+(\mathbf{v}\cdot\boldsymbol{\nabla})\mathbf{v}-\frac{1}{2}\sum_i a_i\partial^2_{ii}\mathbf{v}=-\alpha\tau\boldsymbol{g}-\frac{1}{\rho_0}\boldsymbol{\nabla}P+\nu\nabla^2\mathbf{v}, \tag{12}$$

where ν denotes the kinematic viscosity. First, the formulation is adimensionalized with respect to the time variable $t' = \frac{D_T}{h^2}t$, where h^2/D_T corresponds to the typical time of a thermal diffusion over h, and the spatial variables: $x' = x/h$, $z' = z/h$. The uncertainty ratio Υ, characterizing the order of magnitude of the horizontal turbulent diffusion $a'_x = \Upsilon a_x$, $a'_z = \Upsilon a_z$, is then introduced, together with the temperature deviation $\tau' = \tau/\delta t$. Multiplying the system by $\frac{h^3}{D_T\nu}$ and finally incorporating the dimensionless Prandtl number $Pr a = \frac{\nu}{D_T}$, ratio of the kinematic viscosity to the thermal diffusivity, the Rayleigh number $Ra = \frac{\alpha\delta T g h^3}{\nu D_T}$ and the dimensionless pressure variable $\Pi = \frac{1}{\rho_0}\frac{h^2}{D_T\nu}\partial_{z'}P'$, the following 2D system is obtained (where the prime index has been dropped for sake of clarity):

$$\frac{1}{Pr a}\left(\partial_t \mathbf{v} + (\mathbf{v}\cdot\boldsymbol{\nabla})\mathbf{v} - \frac{1}{2\Upsilon}\sum_i a_i \partial^2_{ii}\mathbf{v}\right) = -\boldsymbol{\nabla}\Pi + \nu\nabla^2\mathbf{v}, \tag{13}$$

$$\mathbb{D}_t\tau - w\mathrm{d}t - \Upsilon^{-1/2}(\boldsymbol{\sigma}\mathrm{d}\boldsymbol{B}_t)_z = \nabla^2\tau\mathrm{d}t.$$

Since $\mathbf{v}(x,z) = (u(x,z), w(x,z))$ is divergence-free, the 2D momentum equations can be written in a vorticity stream function form:

$$\frac{1}{Pr a}\left(\partial_t\nabla^2\Psi + J(\Psi,\nabla^2\Psi) - \frac{1}{2}\frac{1}{\Upsilon}\sum_i a_i\partial^2_{ii}\nabla^2\Psi\right) = Ra\,\partial_x\tau + \nu\nabla^4\Psi, \tag{14}$$

where Ψ denotes the stream function and $J(\Psi,\omega) = \boldsymbol{\nabla}^\perp\Psi\cdot\boldsymbol{\nabla}\omega = \mathbf{v}\cdot\boldsymbol{\nabla}\omega$ denotes the Jacobian of the transformation $\boldsymbol{x} \to (\Psi,\ \omega)^T$ with the 2D vorticity $\omega = \boldsymbol{\nabla}^\perp\cdot\mathbf{v} = -\partial_z u + \partial_x w$. This equation together with the thermal equation describes the whole dynamics of the flow. As for the divergence-free random field, we similarly consider a stream function vector formulation $\boldsymbol{\sigma}\mathrm{d}\boldsymbol{B}_t = \boldsymbol{\nabla}^\perp\boldsymbol{\Psi}_\sigma^T\mathrm{d}\boldsymbol{B}_t$. Note that the kernel, $\breve{\boldsymbol{\Psi}}_\sigma$, of the linear operator $\boldsymbol{\Psi}_\sigma$ is a vector of two components:

$$(\boldsymbol{\Psi}_\sigma^T\mathrm{d}\boldsymbol{B}_t)(\boldsymbol{x}) = \int_\Omega \mathrm{d}\boldsymbol{z}\sum_{k=1}^{2}\left(\breve{\Psi}_\sigma(\boldsymbol{x},\boldsymbol{z})\right)_k(\mathrm{d}\boldsymbol{B}_t(\boldsymbol{z}))_k\,. \tag{15}$$

2.3. Fourier modes projection and simplified solution

The Lorenz model corresponds to a simplified solution of this system, considering a Galerkin projection onto the first Fourier modes coupled with suited boundary conditions. The boundary conditions are $\tau = 0$ at $z = 0, 1$ to get the appropriate fixed temperature on the domain frontiers and $\partial_z u = 0$ and $w = 0$ at $z = 0, 1$, *i.e.* neglecting the shear forces on the boundary. For the random term, we assume periodic boundary conditions for simplicity. Indeed, it is a necessary condition for homogeneity, and thus for a constant diagonal diffusion tensor. These specific boundary conditions may be understood as a random forcing at the domain boundary, and are satisfied by the following ansatz for the streamfunction and the temperature deviation:

$$\tau(x,z,t) = \underbrace{T_1(t)\sin(\pi z)\cos(\ell x)}_{\tau_1}\underbrace{-T_2(t)\sin(2\pi z)}_{\tau_2}, \tag{16}$$

$$\Psi(x,z,t) = \phi(t)\sin(\pi z)\sin(\ell x). \tag{17}$$

The two parts, τ_1 and τ_2 of the temperature fluctuation are random (through T_1 and T_2) and provide the temperature deviation on the fluid parcel boundary and at the parcel center, respectively. To ensure a diagonal diffusion tensor as previously specified, the random

stream function term is defined on the two first Fourier modes and their conjugates :

$$\boldsymbol{\Psi}_\sigma^T \mathrm{d}\boldsymbol{B}_t = \frac{1}{\Upsilon^{1/2}} \sum_{i,j=1}^{2} \left(\cos\left(g_{ij}\right) \mathrm{d}\beta_t^{ij} + \sin\left(g_{ij}\right) \mathrm{d}\zeta_t^{ij}\right), \tag{18}$$

where the phases are given as $g_{ij} = (-1)^i \pi z - (-1)^j \ell x$ and the modulus are defined from the constant $\Upsilon^{-1/2}$ and eight independent scalar Brownian variables $\{\beta_t^{ij}, \zeta^{ij} \colon i,j = 1,2\}$. It may be checked that this representation fits the homogeneity condition:

$$\mathbb{E}\left\{\boldsymbol{\Psi}_\sigma^T(x_1,z_1)\mathrm{d}\boldsymbol{B}_t \boldsymbol{\Psi}_\sigma^T(x_2,z_2)\mathrm{d}\boldsymbol{B}_t\right\} = \frac{1}{\Upsilon} \sum_{i,j=1}^{2} \cos\left((-1)^i \pi(z_1 - z_2) - (-1)^j \ell(x_1 - x_2)\right) \mathrm{d}t. \tag{19}$$

The small-scale random velocity becomes:

$$\begin{aligned} \Upsilon^{1/2} \boldsymbol{\sigma} \mathrm{d}\boldsymbol{B}_t &= \boldsymbol{\nabla}^\perp \boldsymbol{\Psi}_\sigma(x,z)\mathrm{d}\boldsymbol{B}_t \\ &= \sum_{i,j=1}^{2} \begin{pmatrix} (-1)^i \pi \\ (-1)^j \ell \end{pmatrix} \left(\sin(g_{ij})\beta_t^{ij} - \cos(g_{ij})\zeta_t^{ij}\right), \end{aligned} \tag{20}$$

which can be developed in factors of $\cos \times \sin$, $\cos \times \cos$, and $\sin \times \sin$. We may check that the diffusion tensor is then given by

$$\boldsymbol{a} = \frac{1}{\Upsilon} \sum_{i,j=1}^{2} \begin{pmatrix} (-1)^{2i}\pi^2 & (-1)^{i+j}\pi\ell \\ (-1)^{j+i}\pi\ell & (-1)^{2j}\ell^2 \end{pmatrix} = \frac{4}{\Upsilon} \begin{pmatrix} \pi^2 & 0 \\ 0 & \ell^2 \end{pmatrix}. \tag{21}$$

This choice, though simple, remains sufficiently general for our purpose. Factorizing by $\sin(\pi z)\sin(\ell x)$ the ~~barotropic~~ dynamics (14), we immediately infer that the stream function temporal mode, $\phi(t)$, has to satisfy the following differential equation

$$\partial_t \phi(t) = \frac{Pr a Ra T_1(t)}{(\ell^2 + \pi^2)} - (\pi^2 + \ell^2)\left(Pr a + \frac{4}{\Upsilon} \frac{\pi^2 \ell^2}{(\pi^2 + \ell^2)}\right)\phi(t). \tag{22}$$

This equation includes a random forcing term coming from the temperature variation. As for the thermo-dynamical equation, removing the high-order frequency terms, gathering on the one hand the terms in $\sin(\pi z)\cos(\ell x)$ and in the other hand the terms in $\sin(2\pi z)$, and introducing a new scalar Brownian motion $B_t = \frac{1}{2}\sum_{i,j=1}^{2} (-1)^{i+j}\beta_t^{ij}$ (for which it can be easily verified that the quadratic variation is t), we get:

$$\mathrm{d}T_1 + \left(\ell^2 + \pi^2 + \frac{4}{\Upsilon}\pi^2\ell^2\right)T_1(t)\mathrm{d}t - \ell\phi\mathrm{d}t - \frac{\ell}{\Upsilon^{1/2}}\mathrm{d}B_t = -\ell\phi\pi T_2 \mathrm{d}t - \frac{\ell\pi T_2}{\Upsilon^{1/2}}\mathrm{d}B_t, \tag{23}$$

and

$$-\mathrm{d}T_2 - \left(1 + \frac{2}{\Upsilon}\ell^2\right)4\pi^2 T_2 \mathrm{d}t = -\frac{1}{2}\ell\pi\phi T_1 \mathrm{d}t - \frac{1}{2}\frac{\ell\pi T_1}{\Upsilon^{1/2}}\mathrm{d}B_t, \tag{24}$$

respectively.

2.4. *Lorenz system under uncertainty*

To get to the final simplified system, we finally consider the time scale $t' = (\pi^2 + \ell^2)t$, the change of variables:

$$X(t) = \frac{\ell\pi}{(\ell^2+\pi^2)\sqrt{2}}\phi(t), \tag{25}$$

$$Y(t) = \frac{r\pi}{\sqrt{2}}T_1(t), \tag{26}$$

$$Z(t) = \pi r T_2(t), \tag{27}$$

and the reduced Rayleigh number

$$r = \frac{Ra\ell^2}{(\pi^2+\ell^2)^3}. \tag{28}$$

With this time renormalized, the new Brownian variable is $B_{t'} = \sqrt{\pi^2+\ell^2}B_t$. We also note

$$\frac{1}{\tilde{\Upsilon}^{1/2}} = \frac{2}{\Upsilon^{1/2}}\frac{\ell\pi}{\sqrt{\ell^2+\pi^2}\sqrt{2}}. \tag{29}$$

Those changes of variables, with the parameter $b = 4\pi^2/(\pi^2+\ell^2)$, lead to the final system of equations where, for the sake of readability, we kept the notation Υ instead of $\tilde{\Upsilon}$ and dropped the prime index on time:

$$\frac{\mathrm{d}X}{\mathrm{d}t} = Pra\Big(Y - X\Big) - \frac{4}{2\Upsilon}X, \tag{30a}$$

$$\mathrm{d}Y = \Big((r-Z)X - Y - \frac{4}{2\Upsilon}Y\Big)\mathrm{d}t + \frac{r-Z}{\Upsilon^{1/2}}\mathrm{d}B_t, \tag{30b}$$

$$\mathrm{d}Z = \Big(XY - bZ - \frac{8}{2\Upsilon}Z\Big)\mathrm{d}t + \frac{Y}{\Upsilon^{1/2}}\mathrm{d}B_t. \tag{30c}$$

This model constitutes a stochastic version of the Lorenz model. It is composed of a deterministic differential equation on the velocity variable together with two coupled stochastic differential equations associated with the temperature fluctuations. For a negligible noise ($\Upsilon \to \infty$), we recover the original model. Besides, in the Y and Z equations, the noise terms involve the same factors as the advection terms in factor of the velocity variable (X). Hence, they both correspond to the advection of temperature variables by the small-scale velocity. An additive noise component, weighted by the Rayleigh coefficient, is obtained in the Y equation. It corresponds to the random interaction between the small-scale velocity and the stratification δT appearing in (11). This term and its influence on the buoyancy variations has been detailed in Resseguier *et al.* (2017a).

It should be noticed that in this stochastic Lorenz system, the velocity variable is driven by an ordinary differential equation. This is in the first place due to our assumption of a smooth-in-time large-scale velocity. Relaxing this assumption (i.e. considering that the large-scale velocity component depends also on a Brownian variable, which is allowed by our derivation) the expression of the velocity for the Lorenz 63 system would however remains deterministic. As a matter of fact, the multiplicative noise is antisymmetric, and thus described (in an orthonormal basis) by an antisymmetric matrix with a null diagonal. Consequently, the noise would have no effect, as only one Fourier mode is kept in the Lorenz-63 model to represent the velocity. In other words, the noise transfers energy from one mode to the other. If only one mode is considered, the noise has no effect. Nevertheless, the turbulent diffusion is still present as it takes out energy from the resolved mode to transfer it to the truncated modes.

In the three equations and as compared to the original Lorenz system, the diffusion terms are increased by a factor that depends on the noise variance scale Υ. Due to the scale truncation, the energy loss of Y by turbulent diffusion is 4 times larger than the multiplicative noise intake. It is 8 times larger for Z. The stochastic system exhibits a symmetry for $(-X,-Y,Z,-B)$. Thus, the law of the solution is symmetric for $(-X,-Y,Z)$.

To infer the different physical mechanisms, it is usefull to rewrite system (30) with Stratonovich notations (Oksendal 1998):

$$\mathrm{d}\begin{pmatrix} Y \\ Z \end{pmatrix} = \boldsymbol{F}\mathrm{d}t + \Upsilon^{-1/2}\boldsymbol{G}\mathrm{d}B_t = \boldsymbol{F}^*\mathrm{d}t + \Upsilon^{-1/2}\boldsymbol{G}\circ\mathrm{d}B_t, \tag{31}$$

$$\begin{aligned} \text{where } \boldsymbol{F}^* &= \boldsymbol{F} - \frac{1}{2\Upsilon}(\boldsymbol{G}\cdot\boldsymbol{\nabla}_{YZ})\boldsymbol{G}, \\ &= \underbrace{\boldsymbol{G}X}_{\substack{\text{Large-scale}\\ \text{advection}}} - \underbrace{\begin{pmatrix} 1 & 0 \\ 0 & b \end{pmatrix}\begin{pmatrix} Y \\ Z \end{pmatrix}}_{\substack{\text{Molecular}\\ \text{diffusion}}} - \underbrace{\frac{1}{2\Upsilon}\begin{pmatrix} 3 & 0 \\ 0 & 7 \end{pmatrix}\begin{pmatrix} Y \\ Z \end{pmatrix}}_{\substack{\text{Turbulent diffusion due}\\ \text{to scale truncation}}}, \end{aligned} \tag{32}$$

$$\boldsymbol{G} = \begin{pmatrix} r \\ 0 \end{pmatrix} + \begin{pmatrix} 0 & -1 \\ 1 & 0 \end{pmatrix}\begin{pmatrix} Y \\ Z \end{pmatrix}, \text{ and } \boldsymbol{\nabla}_{YZ} = \begin{pmatrix} \partial_Y \\ \partial_Z \end{pmatrix}. \tag{33}$$

Since $\boldsymbol{G}$ represents an advection term, its linear part is antisymmetric and thus has no effect either on the temperature energy Y^2+Z^2 or on the dilation or contraction of the state space ($\boldsymbol{\nabla}_{YZ}\cdot\boldsymbol{G}=0$). However, according to the system's flow Jacobian (Resseguier *et al.* 2017a), the drift term, $\boldsymbol{F}^*$, uniformly shrinks the state space volume:

$$\begin{aligned} V(t) &= V(0)\exp\left(\int_0^t \left(\left(\partial_X\dot{X} + \boldsymbol{\nabla}_{YZ}\cdot\boldsymbol{F}^*\right)\mathrm{d}t + \boldsymbol{\nabla}_{YZ}\cdot\boldsymbol{G}\mathrm{d}B_t\right)\right), \\ &= V(0)\exp\left(-\left(Pra + 1 + b + \frac{7}{\Upsilon}\right)t\right). \end{aligned} \tag{34}$$

Note that the noise term increases the shrinking rate through the turbulent diffusion term induced by the spatial scale truncation. In addition, the random terms are volume-preserving since they have an antisymmetric multiplicative structure as stated by the transport operator (4). More arbitrary choices of multiplicative random Lorenz systems studied in the literature do not necessarily keep such properties Chekroun *et al.* (2011). This key difference between stochastic systems build from a stochastic transport operator and the multiplicative stochastic system studied in Chekroun *et al.* (2011) has also been put forward through the Lyapunov exponents in Geurts *et al.* (2017). While obtained from a different derivation, the stochastic system with noise transport studied in Geurts *et al.* (2017) is close to the system derived from the modeling under location uncertainty.

Additive noise terms in the sytems (Dorfle and Graham 1983) have also been considered. However, those latter models do not correspond to the observed small-scale tracers, which are non-Gaussian and intermittent. Such phenomena are well described in simple scalar advection models with multiplicative random processes (Kraichnan 1968, 1994; Majda and Kramer 1999; Sura *et al.* 2005).

The system expectation (conditionally to the velocity) corresponds to a Lorenz model with an augmented diffusion and hence constitutes a damped version of the deterministic version of the original model. There are still three equilibrium points for $r>1$ located at $(0,0,0)$ $(\pm[(1+\frac{2}{\Upsilon})(b+\frac{4}{\Upsilon})\alpha]^{1/2}, \pm[(b+\frac{4}{\Upsilon})\alpha]^{1/2}, \alpha)$ with $\alpha = (r-(1+\frac{2}{\Upsilon})(1+\frac{2}{\Upsilon Pra}))$. For a small noise variance, we

recover to leading order the usual equilibrium points, but for strong noise, there is a shift due to the large-scale diffusion engendered by the noise.

The classical Lorenz system corresponds to a description of the flow in which the small-scale velocity fluctuations are simply ignored through a truncation on the Fourier space. The diffusions introduced are then only related to the kinematic viscosity and to the thermal diffusivity. The modeling of the small-scale effects as purely dissipative processes, as this is done in Large Eddies Simulation (LES), would introduce stronger diffusions through eddy viscosity and eddy diffusivity coefficients.

The Lorenz system under location uncertainty can thus be interpreted as a coarse time-scale description of the dynamical system in which the intrinsic Lagrangian velocity anomaly is encoded through a temporally uncorrelated random variable. Here, the latter is encoded as a scalar white noise variable depicting an uncertainty on the temporal evolution of the two first Fourier modes of the flow velocity. The velocity anomalies have a characteristic time that is much smaller than the resolved (differentiable) velocity. At the resolution characteristic time, these velocities anomalies can thus be considered as fully decorrelated. One crucial property of such large scale representations concerns the rate at which they tend to the "finest" original system when the noise tends to zero (e.g. when $\Upsilon \to \infty$). We will show in the following section that the proposed stochastic system includes the property to approach the original system for moderates values of Υ and to provide reasonable coarse descriptions for small Υ values. This ability constitute the most striking difference with a diffusive "eddy-viscosity" model, which has a good convergence behavior but yields a wrong representation at high eddy-viscosity value, or with an *ad hoc* stochastic multiplicative forcing approach that appears to have a poor representation property even for low noise.

3. Numerical simulations of large-scale representations

In the following, we consider several simulations of this stochastic Lorenz system. The gold standard to which this system should be compared with, would ideally consist to reconstruct an ensemble of trajectories of an equivalent reduced order model built from a full direct numerical simulation of a Raleigh-Benard convection (with a large number of different initial conditions). This solution would constitute a huge computational effort. Instead of doing that, we will compare the performances of different representations of the Lorenz-63 system with the original system. The deterministic Lorenz system does not constitute per se a gold standard in the sense that it corresponds to a reduced order model that represents the evolution of only the first Fourier modes (one mode for the velocity, two modes for the temperature) with no model for the truncated modes. However these modes capture well – in an ideal setting – the recurrent pattern of the metastable Raleigh-Benard convection cells. A representation of the small-scale effects will not considerably affect the representation of these large scale effects at least in average. Obviously, intermittency and small-scale perturbations will likely modify an instantaneous picture of these cells and of their motion. As a consequence, any Lorenz systems with a representation of the truncated modes should statistically not differ too much from the original Lorenz system. All of them should statistically represent the same large-scale physics. In particular the pdf or the mean spectrum of the system variables at large scale should be close to those of the deterministic Lorenz-63 system. Furthermore beyond its relation with the Raleigh-Benard convection, the Lorenz-63 model is a toy model that reproduces qualitatively essential mechanisms of geophysical dynamics: a temperature advection and a non linearity with a velocity forced by temperature. It is interesting to observe how different modifications introducing multiplicative noise and eddy-diffusion mechanisms depart from the original deterministic system.

We consider the original Lorenz system for the usual chaotic parameters ($P_{ra} = 10, r = 28, b = 8/3$). Its small dimension enables to easily visualize the solution attractor and to obtain empirical probability density function of the phase space. The Lorenz-63 system

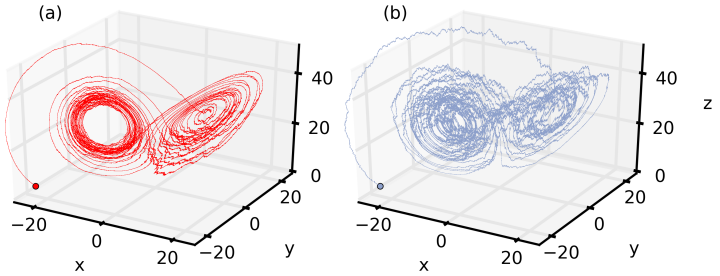

Figure 1. Trajectory of the Lorenz system under location uncertainty (a) and the Basic stochastic Lorenz systems (b) in a strong noise case ($\Upsilon = 10$).

will be termed with the LZ acronym. For the parameter values investigated here, LZ admits an invariant set, over which almost all initial conditions are attracted.

The second system we will consider corresponds to the dissipative system without the noise terms. This latter system can be interpreted as a damped version of LZ. The temporal modes are further damped from a supplementary diffusion term, akin to classical large eddies representations of the dynamics through eddy viscosity subgrid models. Expressed as a spatial diffusion in the physical domain, these subgrid effects are represented by a damping term on the Fourier temporal modes. The action of the unresolved variables on the resolved variables solely results from the dissipative subgrid operator. This system will be denoted LES-LZ.

The third model corresponds to the proposed stochastic model. It includes the previous dissipative terms, but also the multiplicative noise terms borne by the location uncertainty formulation. This system is referred to LUS-LZ – for Location Uncertainty Stochastic Lorenz-63.

A fourth system is empirically defined by adding to LZ, multiplicative noise variables $1/\Upsilon Z dB_t$ and $1/\Upsilon Y dB_t$ on Z and Y variables, respectively. Hence the noise has a diagonal structure and there is here no additional diffusion. This basic stochastic model is termed BS-LZ.

A first remark on the different systems can immediately be done. The stochastic and diffusive systems straightforwardly tend to LZ when the noise (or the diffusion) tend to zero. Yet, the rate at which those modified systems tend to the deterministic system is crucial. In particular, for very small noise condition, it is not desirable to greatly differ from LZ.

For those four systems, simulations with different initial conditions have been carried out. For the two deterministic systems, LZ and the diffusive LES-LZ, an ensemble is engendered by random perturbations of the initial condition. The same point is used to initiate the realizations of the stochastic systems. The noise amplitude and the initial perturbation have been fixed through the scaling Υ. Numerically, the four systems have been set on equal footing. We employed a simple Euler-Maruyama integration for the stochastic differential equations associated with a tiny time step (10^{-5}). To obtain comparable results, an Euler scheme has been used with the same value for the deterministic systems. Several simulations with 100 particles have been run with different noise levels and initial conditions. An example of the trajectories of one realization of the two stochastic systems with the same initial condition and the same level of noise are displayed on Figure 1. The BS-LZ trajectory is rough while the smoother LUS-LZ trajectory is more akin to that of the deterministic LZ.

The curves plotted in Figure (2,3 and 4) show, for two different noise levels, the empirical (marginal) probability distribution and the power spectrum of the variables X, Y and Z, respectively. As immediately noticed, the diffusive Lorenz system for a strong noise ($\Upsilon = 10$) strongly modifies the empirical pdf. Two peaks are now observed at the equilibrium points, located at the center of the attractor wings. The trajectories are more easily trapped in the attraction bassin of these points. Yet, the eddy viscosity coefficient is smaller than one, 1/5 and 2/5 on X and Z, respectively. The spectrum for long time-scale is also modified for the three variables, especially the Z variable. For small diffusion, $\Upsilon = 100$, and eddy viscosity coefficients of $1/50$, $1/50$ and $1/25$ for X Y and Z, respectively, the

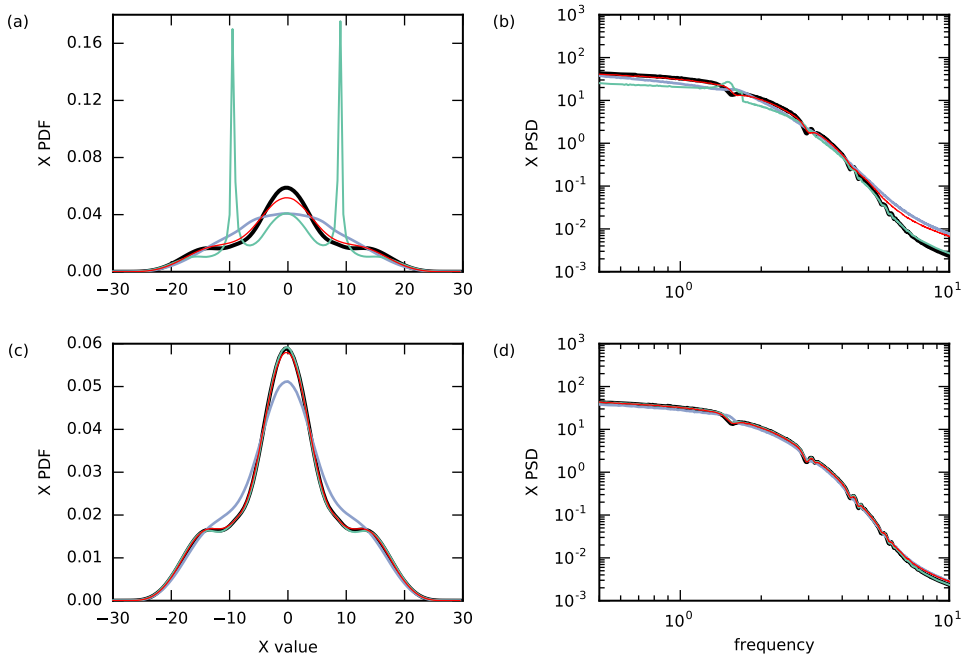

Figure 2. Velocity (X) empirical Pdf (left column) and power spectrum (right column) computed for 10,000 realizations in a strong noise case (first row) and small noise case (second row) respectively. The black line stands for the deterministic Lorenz system, the red line for the Lorenz model under location uncertainty, the green one for a diffusive large scale Lorenz system and the blue one for the basic stochastic system.

pdfs and the power spectra superimpose almost perfectly with pdfs and spectra of the deterministic system. This model converges to the deterministic system for small diffusion. Note, we recover here the common practice in computer fluid dynamics that limits the use of diffusive LES to resolutions quite close to high resolution simulations. At variance, the random empirically forced system (BS-LZ) performs quite badly. Even for small noise, it leads to significant changes for the pdf shapes of the three variables. Strong discrepancies can be observed in the spectrum of the Z variable in the transition regions between frequency peaks (fig. 4). The BS-LZ thus badly converge toward the deterministic system. It constitutes a bad random representation of the original system. Compared to the others, the LUS-LZ still holds well for high noise. Though slightly smoothed, the shapes of the marginal pdf and of the spectra are well preserved at large time scale. Some discrepancies only appear at high frequency where the noise impact is clearly visible.

To quantify the exploration of the Lorenz attractor, we rely on a discrete covering of the usual deterministic attractor made of 611550 cubic boxes of radius $r = 0.15625$, computed with the GAIO software Dellnitz *et al.* (2001). Figures 5 and 6 depict for the LZ, LES-LZ and LUS-LZ systems examples of the attractor's discrete covering visited by an ensemble of realizations started from an initial condition on the attractor. Those maps exemplify the differences between the three systems for a strong noise ($\Upsilon = 10$) (fig. 5) and a small noise ($\Upsilon = 100$) (fig. 6), respectively. In the strong noise case, the diffusive system (fig. 5b) remains stuck in the basin of an equilibrium point. This explains the pdf peaks observed in the upper left panels of figures (2,3 and 4), and also highlights a problematic systematic bias of diffusive large-scale systems toward system's stable states. On the contrary, LUS-LZ (fig. 5c) visits a much larger part of the attractor. The shape of the visited part of the attractor is similar to the set of points explored by LZ (fig. 5a), though the stochastic system seems to visit the attractor in a faster way. At small noise, the three maps are similar (fig. 6). However, surprisingly enough, the stochastic system still seems to visit more rapidly the attractor. It rapidly escapes the equilibrium basin, whereas the LES-LZ (fig. 6b) remains near the equilibrium point. The LZ (fig. 6a) succeeds to visit both attractor wings, but in a less efficient way than the stochastic system does.

Those experiments have been generalized for 100 random different initial conditions (still on the attractor) of the 100-particles ensemble (which amounts to 10,000 realizations). The results are displayed fig. 7 in the strong and low noise case, respectively. for the

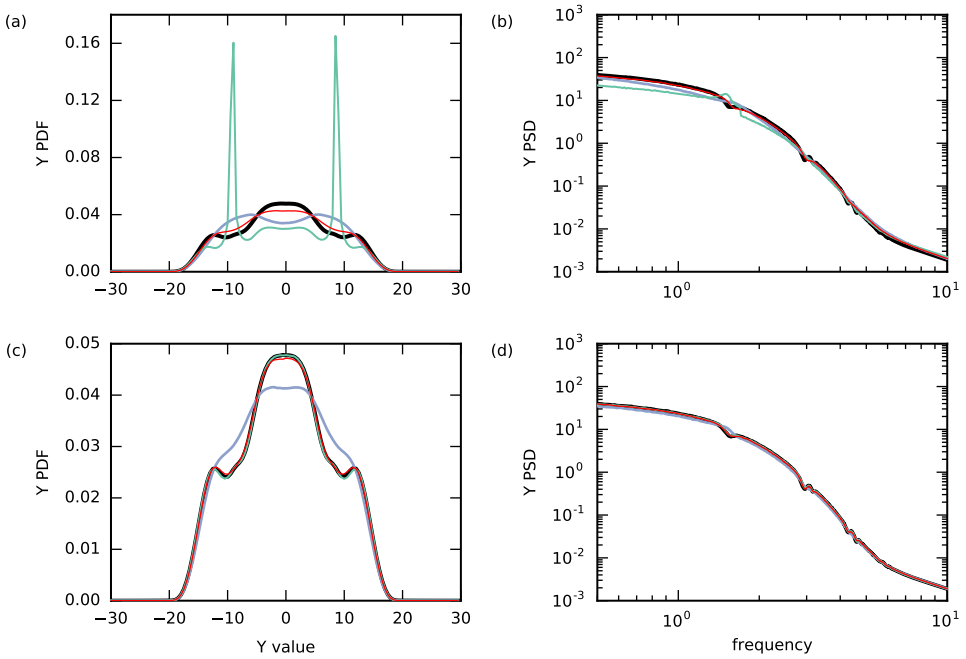

Figure 3. Velocity (Y) empirical Pdf (left column) and power spectrum (right column) computed for 10,000 realizations in a strong noise case (first row) and small noise case (second row) respectively. The black line stands for the deterministic Lorenz system, the red line for the Lorenz model under location uncertainty, the green one for a diffusive large scale Lorenz system and the blue one for the basic stochastic system.

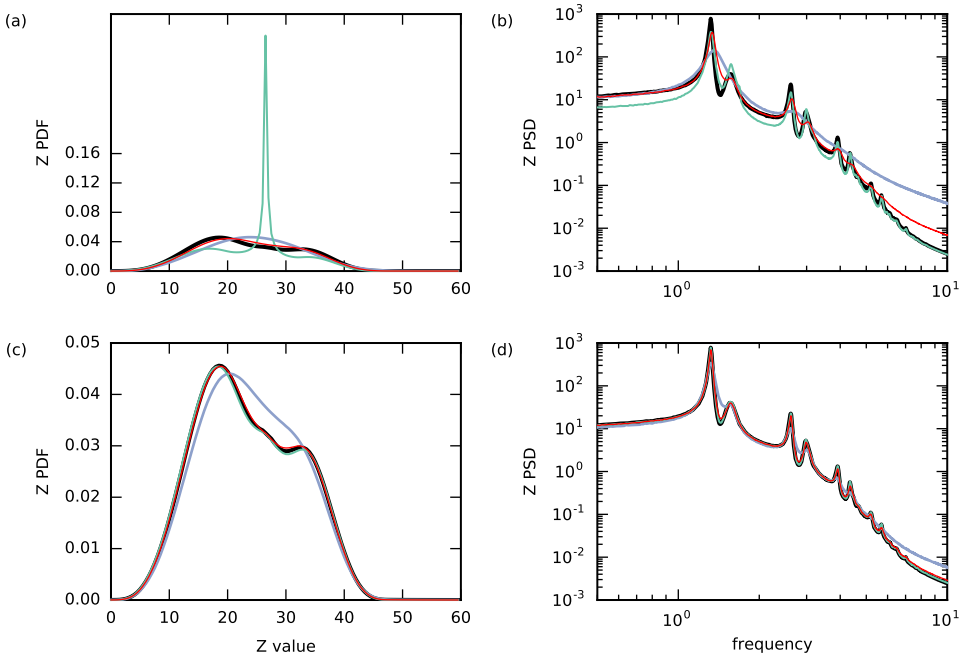

Figure 4. Velocity (Z) empirical Pdf (left column) and power spectrum (right column) computed for 10,000 realizations in a strong noise case (first row) and small noise case (second row) respectively. The black line stands for the deterministic Lorenz system, the red line for the Lorenz model under location uncertainty, the green one for a diffusive large scale Lorenz system and the blue one for the basic stochastic system.

average visit rate, computed over 100 ensembles, of the attractor. For a given ensemble of 100 particles, the rate of visit τ as a function of time t is defined as:

$$\tau(t) = \frac{\#\{\text{boxes visited by 100 particles over time } [0;t]\}}{\#\{\text{boxes covering the attractor}\}} \tag{35}$$

In the strong noise case, the visiting rate significantly differs for the three systems. As previously observed, the LES-LZ shows some difficulties to efficiently explore the attractor. A significant part of the trajectories remains close to the equilibrium points. On average,

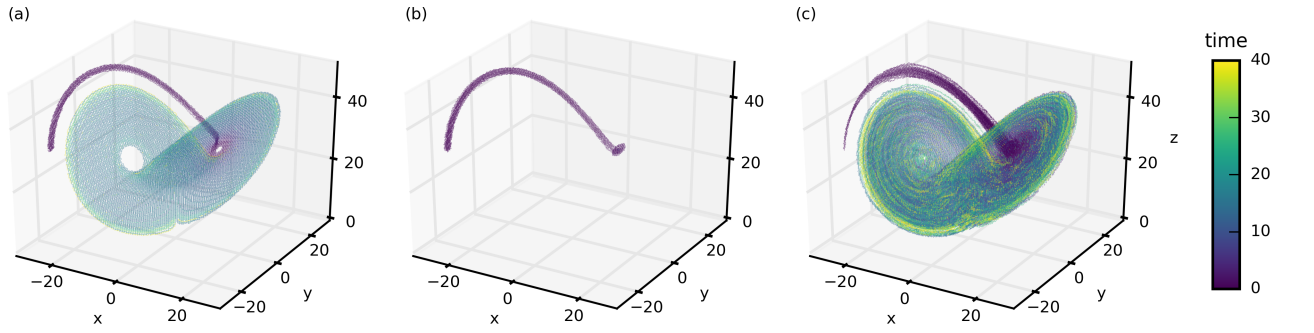

Figure 5. Attractor's points visited by 100-particles ensembles initialized with the same random initial condition (strong noise case $\Upsilon = 10$) for $t \in [0, 40]$ for the deterministic Lorenz system (a), the diffusive "LES-LZ" Lorenz system (b) and the "LUS-LZ" stochastic Lorenz system under location uncertainty " (c). The color encodes the time necessary to reach a given point of the attractor for the first time.

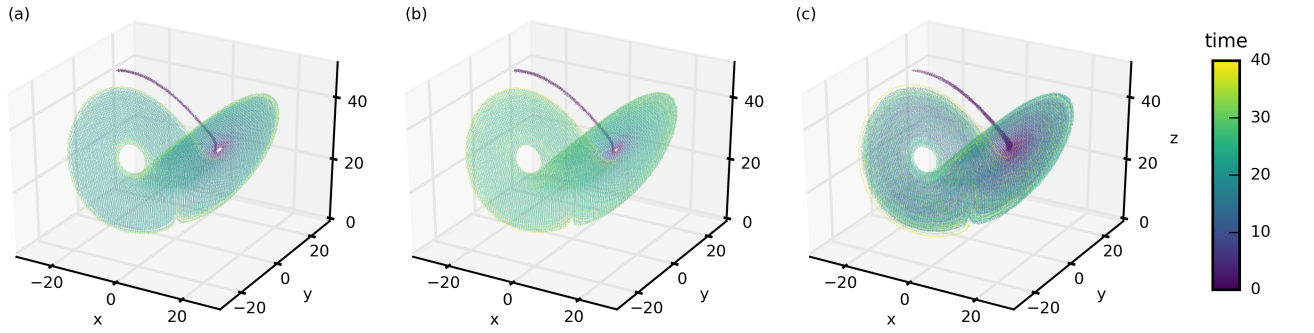

Figure 6. Attractor's points visited by 100-particles ensembles initialized with the same random initial condition (strong noise case $\Upsilon = 100$) for $t \in [0, 40]$ for the deterministic Lorenz system (a), the diffusive "LES-LZ" Lorenz system (b) and the "LUS-LZ" stochastic Lorenz system under location uncertainty (c). The color encodes the time necessary to reach a given point of the attractor for the first time.

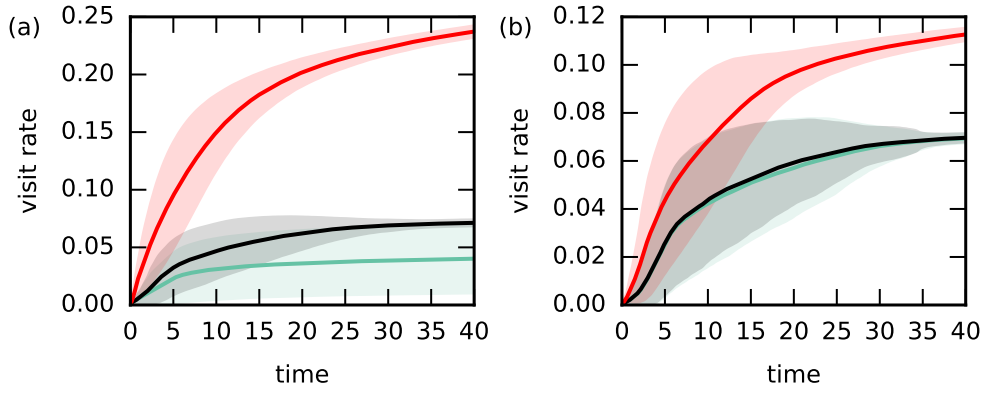

Figure 7. Mean attractor visiting rate (see text) up to $t = 40$ computed for 10,000 realizations (100 ensembles of 100 particles) for the deterministic Lorenz system (black); the diffusive "LES-LZ" Lorenz system (green) and the "LUS-LZ" stochastic Lorenz under location uncertainty " (red); the $\pm$ standard deviations are superimposed in lighter color: (a) strong noise case; (b) small noise case.

less than 5% of the attractor has been visited at time $t = 40$. The LZ system certainly performs better, but several configurations remains in the equilibrium basin. On average, about 7% of the attractor have been explored in the same lapse of time. The stochastic system provides much better results. It enables to explore a much greater part of the attractor (nearly 25% in average) for the same number of realizations. In the small noise case, as could have been anticipated, the LES-LZ results are much closer to the LZ one. It can be noted that almost the same portion of the attractor, as in the strongly perturbed case, have been explored by both LES-LZ and LZ. Therefore a stronger perturbation of the initial condition of the classical Lorenz system only results in a small increase of the attractor visit. The standard deviation associated to the deterministic systems (LES-LZ and LZ) is not significantly strengthened by a strong perturbation of the initial condition. The LUS-LZ, even in a small noise configuration, shows a remarkable ability to visit a larger portion of the attractor ($> 10\%$).

It can be noticed that for LUS-LZ and LZ the variance of the visiting rate grows rapidly at short time while it strongly decreases at the end of the temporal window. The large variance increase at the beginning is connected to the different initial conditions (randomly drawn on the attractor). Some ensembles will reach the regions of bifurcation of the attractor more rapidly than others, depending on where they have been started. When visiting these regions, particles of a given ensemble are sent to very different trajectories. Therefore, for such ensembles, the visiting rate increases rapidly at short time. Other ensembles will take longer to reach the bifurcations, their particles stay close together for a longer time and the visiting rate increases slowly. But, given enough time and for both models, most ensembles go through the bifurcations, spread and explore a similar amount of the attractor – the initial condition has been forgotten – and the variance of the visiting rate decreases. The stochastic model is advantaged by the noise and continues to explore faster than the deterministic one even in a low noise context (the mean visit rate for LUS-LZ increases faster than that of LZ at T = 40). At the end of temporal window, the variance of LUS-LZ remains also higher than the variance of LZ, especially for strong noise. For high diffusion the LES-LZ keeps a high variance as some trajectories remain stuck in the attraction bassin of the equilibrium points.

Conclusion

As considered for this reduced system, the proposed stochastic strategy demonstrates great potential to model geophysical flows. The resulting stochastic system helps to very efficiently explore the entire dynamical landscape of the flows. Without considering a large computational load, a traditional diffusive setting appears more hazardous to use. This is especially true when a significant diffusion is studied. In that case, a purely diffusive subgrid model shows limited performances, and implies supplementary computational efforts. It rapidly reaches the burdens of almost fully resolved systems ! As rigorously derived, the stochastic strategy helps to avoid eventual pitfalls leading to strongly biased scenarios from insufficient exploration of the phase space dynamics. As also tested, the addition of an empirical stochastic forcing barely constitutes an acceptable solution, as possibly leading to a bad representation of the target system. From these results, it thus appears mandatory to more systematically promote the derivation of proper stochastic representations of the classical geophysical systems for climatic analysis of geophysical flows, following geometric mechanics and variational principle Holm (2015), or the location uncertainty formalism as developed here above.

Acknowledgements

The authors are very grateful to Dan Crisan and Darryl Holm for valuable discussions on this work. We also acknowledge the support of the ESA DUE GlobCurrent project, the “Laboratoires d’Excellence” CominLabs, Lebesgue and Mer through the SEACS project.

References

Berge P, Pomeau Y, Vidal C. 1987. *Order within chaos: Towards a deterministic approach to turbulence.* John Wiley & Sons: New York.

Berner J, Achatz U, Batte L, Camara ADL, Crommelin D, Christensen H, Colangeli M, Dolaptchiev S, Franzke C, Friederichs P, Imkeller P, Jarvinen H, Juricke S, Kitsios V, Lott F, Lucarini V, Mahajan S, Palmer TN, Penland C, Storch JSV, Sakradzija M, Weniger M, Weisheimer A, Williams PD, Yano JI. 2017. Stochastic parameterization: Towards a new view of weather and climate models. *Bull. Amer. Meteor. Soc.* **98**(3): 565–588.

Boussinesq J. 1877. Essai sur la th?orie des eaux courantes. Mémoires présentés par divers savants à l’Académie des Sciences, 23 (1): 1–680.

Chekroun M, Simonnet E, Ghil M. 2011. Stochastic climate dynamics: Random attractors and time-dependent stochastic climate dynamics: Random attractors and time-dependent invariant measures. *Physica D* **240**: 1685–1700.

Cotter C, Gottwald G, Holm D. 2017. Stochastic partial differential equations as a diffusive limit of deterministic Lagrangian multi-time dynamics. Technical report, arXiv:1706.00287.

Crisan D, Flandoli F, Holm D. 2017. Solution properties of a 3d stochastic Euler fluid equation. Technical report, arXiv:1704.06989.

Dellnitz M, Froyland G, Junge O. 2001. The algorithms behind gaio—set oriented numerical methods for dynamical systems. In: *Ergodic theory, analysis, and efficient simulation of dynamical systems*, Springer, pp. 145–174.

Dorfle M, Graham R. 1983. Probability density of the Lorenz model. *Phys. Rev. A* **27**: 1096–1105.

Franzke C, O'Kane T, Berner J, Williams P, Lucarini V. 2015. Stochastic climate theory and modeling. *Wiley Interdisciplinary Reviews: Climate Change* **6**(1): 63–78.

Geurts B, Holm D, Luesink E. 2017. Stochastic transport v fluctuation-dissipation noise in lorenz 63. Technical report, arXiv:1706.05882.

Holm D. 2015. Variational principles for stochastic fluid dynamics. *Proc. R. Soc. A* **471**(ISSN: 1364-5021).

Kraichnan R. 1968. Small-scale structure of a scalar field convected by turbulence. *Physics of Fluids (1958-1988)* **11**(5): 945–953.

Kraichnan R. 1994. Anomalous scaling of a randomly advected passive scalar. *Physical review letters* **72**(7): 1016.

Lorenz E. 1963. Deterministic nonperiodic flow. *J. of atmos. Sci.* **73**(12): 130–141.

Majda A, Kramer P. 1999. Simplified models for turbulent diffusion: Theory, numerical modelling, and physical phenomena. *Physics report* **314**: 237–574.

Mémin E. 2014. Fluid flow dynamics under location uncertainty. *Geophysical & Astrophysical Fluid Dynamics* **108**(2): 119–146, doi:10.1080/03091929.2013.836190.

Oksendal B. 1998. *Stochastic differential equations*. Spinger-Verlag.

Reeks M. 1983. The transport of discrete particles in inhomogeneous turbulence. *J. Aerosol Sci.* **14**(6): 729–739.

Resseguier V, Mémin E, Chapron B. 2017a. Geophysical flows under location uncertainty, part I: Random transport and general models. *Geophysical & Astrophysical Fluid Dynamics* **111**(3): 149–176.

Resseguier V, Mémin E, Chapron B. 2017b. Geophysical flows under location uncertainty, part II: Quasi-geostrophic models and efficient ensemble spreading. *Geophysical & Astrophysical Fluid Dynamics* **111**(3): 177–208.

Resseguier V, Mémin E, Chapron B. 2017c. Geophysical flows under location uncertainty, part III: SQG and frontal dynamics under strong turbulence. *Geophysical & Astrophysical Fluid Dynamics* **111**(3): 209–227.

Resseguier V, Mémin E, Heitz D, Chapron B. 2017d. Stochastic modelling and diffusion modes for proper orthogonal decomposition models and small-scale flow analysis. *J. of Fluid Mech.* **828**: 888–917.

Smagorinsky J. 1963. General circulation experiments with the primitive equation: I. the basic experiment. *Monthly Weather Review* **91**: 99–165.

Sura P, Newman M, Penland C, Sardeshmukh P. 2005. Multiplicative noise and non-gaussianity: A paradigm for atmospheric regimes? *J. of Atmos. Sc.* **62**: 1391–1409.